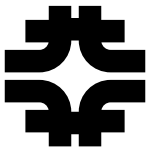

Fermi National Accelerator Laboratory

FERMILAB-Pub-95/410-E
E687

Charm-Anticharm Asymmetries in High Energy Photoproduction

P.L. Frabetti et al.
The E687 Collaboration

Fermi National Accelerator Laboratory
P.O. Box 500, Batavia, Illinois 60510

January 1996

Submitted to *Physics Letters B*

Operated by Universities Research Association Inc. under Contract No. DE-AC02-76CHO3000 with the United States Department of Energy

Disclaimer

Charm-Anticharm Asymmetries in High Energy Photoproduction

The E687 Collaboration

P. L. Frabetti
Dip. di Fisica dell'Università and INFN - Bologna, I-40126 Bologna, Italy

H. W. K. Cheung[a], J. P. Cumalat, C. Dallapiccola[b], J. F. Ginkel, W. E. Johns[c], M. S. Nehring[d]
University of Colorado, Boulder, CO 80309, USA

J. N. Butler, S. Cihangir, I. Gaines, P. H. Garbincius, L. Garren, S. A. Gourlay, D. J. Harding, P. Kasper, A. Kreymer, P. Lebrun, S. Shukla, M. Vittone
Fermilab, Batavia, IL 60510, USA

S. Bianco, F. L. Fabbri, S. Sarwar, A. Zallo
Laboratori Nazionali di Frascati dell'INFN, I-00044 Frascati, Italy

R. Culbertson[e], R. W. Gardner, R. Greene[f], J. Wiss
University of Illinois at Urbana-Champaign, Urbana, IL 61801, USA

G. Alimonti, G. Bellini, M. Boschini, D. Brambilla, B. Caccianiga, L. Cinquini[g], M. Di Corato, M. Giammarchi, P. Inzani, F. Leveraro, S. Malvezzi, D. Menasce, E. Meroni, L. Moroni, D. Pedrini, L. Perasso, F. Prelz, A. Sala, S. Sala, D. Torretta[a]
Dip. di Fisica dell'Università and INFN - Milano, I-20133 Milan, Italy

D. Buchholz, D. Claes[h], B. Gobbi, B. O'Reilly[g]
Northwestern University, Evanston, IL 60208, USA

J. M. Bishop, N. M. Cason, C. J. Kennedy[i], G. N. Kim[j], T. F. Lin, D. L. Puseljic[k], R. C. Ruchti, W. D. Shephard, J. A. Swiatek[l], Z. Y. Wu[m]
University of Notre Dame, Notre Dame, IN 46556, USA

V. Arena, G. Boca, C. Castoldi, G. Gianini, S. P. Ratti, C. Riccardi, L. Viola, P. Vitulo
Dip. di Fisica Nucleare e Teorica dell'Università and INFN - Pavia, I-27100 Pavia, Italy.

A. Lopez
University of Puerto Rico at Mayaguez, PR 00709, Puerto Rico

G. P. Grim, V. S. Paolone, P. M. Yager
University of California-Davis, Davis, CA 95616, USA

J. R. Wilson
University of South Carolina, Columbia, SC 29208, USA

P. D. Sheldon
Vanderbilt University, Nashville, TN 37235, USA

F. Davenport
University of North Carolina-Asheville, Asheville, NC 28804, USA

G.R. Blackett, K. Danyo, M. Pisharody, T. Handler
University of Tennessee, Knoxville, TN 37996, USA

B. G. Cheon, J. S. Kang, K. Y. Kim
Korea University, Seoul 136-701, Korea

Abstract

We report measurements of charm particle production asymmetries from the Fermilab photoproduction experiment E687. An asymmetry in the rate of production of charm versus anticharm particles is expected to arise primarily from fragmentation effects. We observe statistically significant asymmetries in the photoproduction of D^+, D^{*+} and D^0 mesons and find small (but statistically weak) asymmetries in the production of the D_s^+ meson and the Λ_c^+ baryon. Our inclusive photoproduction asymmetries are compared to predictions from nonperturbative models of charm quark fragmentation.

PACS numbers: 13.60.Le, 13.60.Rj

From a data sample of approximately 55000 charm particle decays obtained using silicon vertex detectors and a forward multiparticle spectrometer, we have investigated the production asymmetry between charm and anticharm hadrons produced by the interaction of high energy photons with a Beryllium target. The data were recorded by the E687 Collaboration during the 1990-91 fixed target run at Fermilab.

In high energy photon-hadron collisions charm quarks are expected to be predominantly produced through the photon-gluon fusion process [1]. This mechanism, which is calculated in perturbative QCD at leading order in $\alpha_{em}\alpha_s$, leads to the production of a charm-anticharm quark pair where each member of the pair is distributed identically (on average) in the kinematic variables Feynman-x (x_f) and squared transverse momentum (p_t^2). Contributions from processes occurring at next to leading order in α_s, such as initial and final state gluon bremsstrahlung, have been calculated [2–4] but kinematic asymmetries between the charm and anticharm quarks arising from these processes are expected to be negligibly small. As the charm quarks fragment into colorless charm hadrons, however, nonperturbative effects may induce an asymmetry between charm and anticharm hadron species. To provide a context for discussion, in this paper we will consider the Lund string fragmentation model applied to the photoproduction process as depicted in Fig. 1. In this model the struck gluon leaves the target nucleon in a color octet state which can be divided into a color antitriplet pole (which we will refer to as the "diquark") and color triplet pole (which we will refer to as the "bachelor quark"). The color field between the target diquark and the charm quark, and the field between the target bachelor quark and anticharm quark, are treated as strings having uniform energy per unit length corresponding to a linear confinement potential. The two strings are broken into $q\overline{q}$ pairs (or diquark-antidiquark pairs) resulting in a final state configuration of colorless hadrons (more details of the model can be found in Refs. [5]). We have found that predictions for charm particle production asymmetries generated by this model depend sensitively on the kinematic region probed and on the assumed distribution

for the momentum fraction carried by the bachelor quark. A common assumption,* which we will refer to as "Model 1", is that the bachelor quark carries a fraction χ of the target nucleon's momentum which is sharply peaked towards small values of χ

$$\frac{dN}{d\chi} \sim \frac{(1-\chi)^3}{\chi} \quad (\text{"Model 1"}). \tag{1}$$

By contrast another option uses a "hard" distribution (which we will refer to as "Model 2")

$$\frac{dN}{d\chi} \sim 2(1-\chi) \quad (\text{"Model 2"}) \tag{2}$$

which naively assigns on average 1/3 of the nucleon remnant momentum to the bachelor quark. In both cases the remainder of the nucleon remnant momentum is assumed to be carried by the diquark. The kinematics of the charm quark (anticharm quark) and target diquark (bachelor quark) system control the invariant mass acquired by the string which in turn influences which charm species can be produced and also the spectra of "fragmentation" particles which remain at the primary (production) vertex.

The dynamics of the string breaking can potentially lead to a difference in both the overall production rate for a species containing a charm or anticharm quark as well as differences in their kinematic distributions. An example of an overall production asymmetry in photoproduction on a fixed baryon target is the "associated production" of a $\overline{D}$ meson opposite a Λ_c^+ baryon near threshold [7]. A purely kinematic asymmetry, on the other hand, would be observed if, for example, the x_f distribution of D^- mesons was harder than that for D^+ in photoproduced D^+D^- pair events.

It is very difficult to experimentally distinguish between these two forms of asymmetry since experiments can only perform asymmetry measurements in the kinematic domain where they have reasonable acceptance. As we discuss below, the fragmentation affects the charm-anticharm asymmetry as well as the composition of the photoproduced primary vertex which in turn influences the efficiency for isolating charm particles from background by

*This is the default option in the PYTHIA 5.6 Monte Carlo event generator program [6].

lifetime tagging techniques. For this reason we have chosen to compare observed asymmetries directly to model predictions without correcting for acceptance due to apparatus and selection cuts. In the absence of a possible detection asymmetry in our apparatus, which we confirmed was negligible (discussed below) using unbiased non-charm data and Monte Carlo simulations of charm and anticharm quarks fragmented into hadrons according to a symmetric model,[†] any observed charm-anticharm asymmetry is necessarily the result of physical processes such as those discussed here.

The E687 apparatus, beam and trigger were designed to detect charm particles produced in the forward 100 milliradians of the event corresponding to roughly half of the center of mass solid angle. We briefly review the important features for this analysis (complete descriptions can be found in Refs. [9]). Charged particles emerging from photon-Beryllium target interactions are tracked by a microvertex detector consisting of 12 planes of silicon microstrips which allow secondary vertices to be separated from the primary (production) vertex. Downstream (vertical) deflections by two analysis magnets of opposite polarity are measured by five stations of proportional wire chambers (PWCs). Pions, kaons and protons are identified by three multicell Čerenkov counters operating in threshold mode. The photon beam is derived from electrons of approximately 320 GeV/c momentum with a spread of roughly $\pm$ 15%. These electrons impinge on a 27% radiator producing a broad bremsstrahlung photon beam ($< E_\gamma > \simeq$ 200 GeV for events containing charm particle candidates) which is tagged by measuring the incident and recoil electron beam momenta and the energy from extra photons created by multiple bremsstrahlung collisions in the radiator.

The charm particles we investigated are from the high statistics D meson decays $D^+ \to K^-\pi^+\pi^+$, $D^0 \to K^-\pi^+, D^0 \to K^-\pi^+\pi^+\pi^-$ and the less copiously produced D_s^+ meson and

---

[†]For this purpose we used an event generator which independently fragmented the charm and anticharm quarks according to the formalism of Peterson *et al.* [8].

Λ_c^+ baryon observed in the final states $D_s^+ \to K^-K^+\pi^+$ and $\Lambda_c^+ \to pK^-\pi^+$. The signals were extracted using our standard candidate driven vertexing algorithm [9] which identified the primary and secondary vertices of the event. The principal cut influenced by fragmentation is the significance of detachment of the vertices, ℓ/σ_ℓ, which is defined as the distance (ℓ) between the two vertices divided by the error (σ_ℓ) on ℓ.[‡] Additional particle identification cuts were applied: the kaon candidate track in each of the modes was required to be consistent with a Čerenkov hypothesis corresponding to a kaon or ambiguous between a kaon or proton, while for the $\Lambda_c^+ \to pK^-\pi^+$ decay the proton was required to have a Čerenkov hypothesis consistent with that for a proton or ambiguous with being either a kaon or proton. For some of the modes, vertex isolation cuts were applied in order to maximize the apriori sensitivity of the asymmetry measurement. We removed the significant ($\approx 25\%$) contamination of the $D_s^+ \to K^+K^-\pi^+$ signal due to Čerenkov misidentified background from the decay mode $D^+ \to K^-\pi^+\pi^+$ by employing an "anti-reflection" cut which rejected events whose $K^-\pi^+\pi^+$ mass was within 2σ of our reconstructed D^+ mass. For both of the D^0 topologies we separate those which were found to be consistent with being produced through the decay reaction $D^{*+} \to D^0\pi^+$ ("D^*-tag" events) from those inconsistent with that hypothesis ("no D^*-tag" events). An event was classified as D^*-tag if the associated soft pion from the decay was found in the primary vertex, and, when combined with the D^0, formed a $D^{*+} - D^0$ mass difference within 2 MeV/c^2 of the accepted value [10]. Approximately 5% of the "D^*-tag" events contain a background D^0 which was directly produced or from a D^{*0} decay, while approximately 20% of the "no D^*-tag" D^0 events come from a D^{*+} decay (due to efficiency loss in reconstructing the associated cascade pion). Additionally, D^{*+} events will contribute to the D^+ mode and D^{*0} events will contribute to the D^0 modes, though in this analysis we make no attempt to separate these contributions. The invariant mass distributions for

---

[‡]The values for the detachment cuts were (in the order of decay modes listed in Table I): $\ell/\sigma_\ell > 8, 2, 5, 5, 8, 8, 5$.

the decay modes (along with the measured signal yields which were determined by fitting the distributions to a Gaussian function for the signal peak over a polynomial background) are shown in Fig. 2. To indicate the kinematic region of good acceptance, in Fig. 2 we also plot the combined apparatus acceptance and efficiency of selection cuts as a function of x_f for the D meson samples.

The results given below are compared to Monte Carlo simulations [11] based on the Lund event generator programs PYTHIA 5.6 and JETSET 7.3 which, for the processes considered here, contain the leading order photon-gluon fusion matrix element for the production of the charm quarks, the Lund model of string fragmentation for the hadronization of the charm quarks into charm hadrons, and either of the two models discussed above for the bachelor quark momentum fraction χ. Studies of this Monte Carlo program were given in our previous analysis [12] of correlations between pairs of fully and partially reconstructed charm particles. We found that for two of the correlations studied there, the p_t^2 of the $D\overline{D}$ pair and the transverse angle between the D and $\overline{D}$ momentum directions $\Delta\phi$ (acoplanarity angle), the distributions of the data tended to somewhat broader than the model predictions. However, for two other correlations, the invariant mass of the $D\overline{D}$ pair $M_{D\overline{D}}$ and the rapidity difference ΔY between the D and $\overline{D}$ along the incident photon beam direction, the model tended to describe the data reasonably well. We found that Monte Carlo predictions for these correlations exhibit negligible dependence on the assumed model for the bachelor quark χ distribution. Similarly, our Monte Carlo studies show that predictions from either model for the inclusive p_t^2 spectra and the total momentum of the charm candidates are in good agreement with our measurements.

The production asymmetry can be expressed as the difference between the number of detected charm and anticharm particles divided by the sum

$$\alpha = \frac{N_c - N_{\overline{c}}}{N_c + N_{\overline{c}}} \tag{3}$$

where the event yields N_c and $N_{\overline{c}}$ are determined by fitting the invariant mass distributions separated into charge conjugate states. This expression would be equivalent to one in which

the event yields were replaced by absolute cross sections only if the detection efficiencies for charm and anticharm species were equal, the produced charm and anticharm events were (on average) symmetrically distributed in kinematic variables, and if the acceptance corrections were completely free of production model assumptions. However, Monte Carlo studies of the production characteristics for charm particles inclusively generated with the two models considered here indicate the production asymmetry is a strong function of the observed kinematic variables[§] In addition, we found the efficiencies of the vertex cuts employed to extract the charm signals from background depend sensitively on the assumed fragmentation model. This dependence results from the observation that different fragmentation models lead to differing spectra of fragmentation tracks at the production vertex. These tracks (and their measurement errors) are used to identify the production vertex and compute the significance of decay length ℓ/σ_ℓ for the charm candidate. For example, replacing the Lund-based "Model 1" event generator with the symmetric charm-anticharm production Monte Carlo discussed previously, results in absolute acceptance changes of approximately $15-20\%$ which is an unacceptable systematic error if the value of the true production asymmetry is of order a few percent. This effect led to our decision to report asymmetries which have not been corrected for acceptance and compare our results to the model predictions after subjecting the Monte Carlo events through our apparatus and photon beam simulations.

In Table I we list the observed asymmetries α computed according to Eqn. 3 and have compared them to predictions from the two Monte Carlo models. We emphasize that the Monte Carlo events were subjected to the same apparatus conditions, event selection criteria, and analysis cuts as were the data and therefore should correspond to the same range

---

[§]We define the kinematic variables in terms of the incident photon energy (E_γ), the transverse momentum-squared of the charm particle (p_t^2), and the charm particle x_f taken as the ratio of the longitudinal momentum of the charm particle relative to its maximum value evaluated in the photon-nucleon center of momentum frame.

of kinematic variables. Since these reported asymmetries depend on the kinematic region probed, they are valid for the selection criteria described here; alternative criteria, for example those which would effectively induce a momentum selection bias, could change these values.

We considered two sources of systematic error in these measurements. The first was the assumed background shape in the fit to the invariant mass distribution to determine the yields of charm and anti-charm particles; this uncertainty was found to be negligible. The second was any error associated with possible charge asymmetries induced by our detection apparatus. For this purpose we studied the combined responses of the microstrip detectors and PWC system to positively and negatively charged particles using a copious sample of non-charm photoproduced hadronic events. In all cases the pattern of accepted tracks were well reproduced by the Monte Carlo simulation of the E687 spectrometer. To check that the complete reconstruction of "charm-like" vertices did not result in a false asymmetry, a Monte Carlo test was performed using the symmetric charm-anticharm production event generator and the entire measurement process was simulated. The resulting simulated measurements yielded no significant false asymmetry. From these studies we conclude that any systematic error from an apparatus induced asymmetry is negligible compared to our reported statistical errors.

A negative asymmetry for D meson production would be consistent with expectations for some of the $\overline{D}$ mesons being produced opposite Λ_c^+ baryons, or for a kinematic effect induced by the color confinement in the fragmentation process, or some combination of these mechanisms. However, as we have noted, the observation of a negative inclusive asymmetry alone cannot distinguish between these two possibilities. In fact, small negative asymmetries for each of the D mesons are observed which agree in sign with both of the model predictions considered although they have significantly smaller magnitude than those from Model 1 which is characterized by the soft bachelor quark χ distribution sharply peaked near zero. The values predicted by Model 2, which assumes a hard χ distribution, better reproduces the pattern of our measurements for the D mesons. We point out that the models yield

differing production asymmetry values for the two D^0-(no D^*-tag) modes considered here while for the data the asymmetry measurements are consistent. This dependence on decay mode reflects the sensitivity of the model predictions to the kinematic region probed which is different (owing to acceptance and cut selection efficiency) for the no D^*-tag $D^0 \to K^-\pi^+$ and $D^0 \to K^-\pi^+\pi^+\pi^-$ modes. Small but statistically insignificant positive asymmetries are observed for the D_s^+ meson and Λ_c^+ baryon though it is interesting that the two models yield significantly different predictions for the Λ_c^+ production asymmetry.

We emphasize again that the inclusive photoproduction asymmetry measurements reported here depend on the apparatus acceptance and event selection criteria and are therefore experiment-dependent. It is however instructive to compare our results to previous inclusive photoproduction asymmetry measurements from experiments utilizing a forward multiparticle spectrometer and lifetime tagging techniques. In Table II we compare our results to those from the Tagged Photon Collaboration (E691) [13] which used a photon beam with an average energy of approximately 120 GeV. For comparison we have converted our results from an asymmetry (as defined in Eqn. 3) to an antiparticle-particle production ratio $R = N_{\overline{c}}/N_c$ as used by the E691 experiment. Additional measurements of the charm photoproduction asymmetry come from the NA14/2 Collaboration [14] which used a photon beam with average energy of approximately 100 GeV. They reported a combined asymmetry of $\alpha = -0.03 \pm 0.05$ for photoproduced D^+ and D^{*+} mesons, and $\alpha = 0.24 \pm 0.17$ for D_s^+ mesons. By contrast, the SLAC Hybrid Facility Photon Collaboration [7], using a 20 GeV photon beam (and therefore closer to charm threshold), found an excess production of $\overline{D}$ mesons (75 events) over D mesons (23 events) and attributed this excess to associated $\Lambda_c^+\overline{D}$ production. They reported an indirect cross section ratio $\sigma_{\overline{D}\Lambda_c^+}/\sigma_{\rm charm} = (71 \pm 11 \pm 6)\%$. Our results do not significantly differ from the higher energy experiments although we emphasize that the accepted kinematic regions sampled by each experiment may differ significantly and thus the observed asymmetries, owing to the mechanisms discussed above, may not necessarily be equal.

It is therefore interesting to investigate the kinematical variations of the inclusive pro-

duction asymmetry as a function of E_γ, p_t^2 and x_f. For each distribution we fit the invariant mass distributions for particle and antiparticle states divided into bins of that kinematic variable. The kinematic variations for the $D^+ \to K^-\pi^+\pi^+$ decay mode (having superior combined signal-to-background ratio and event statistics of the modes considered) are shown in Fig. 3 where again we have compared our measurements to predictions from the two Monte Carlo models. In each case the Monte Carlo prediction follows the trend observed in data but Model 1, which is characterized by a χ distribution sharply peaked near zero, tends to over-emphasize the behavior. Model 2, which has a hard χ distribution, provides a good description of the kinematic variation we observe with our data sample. Both models predict similar, but more severe, kinematic trends prior to the imposition of acceptance cuts. While the two models provide different predictions for the production asymmetry, very little difference is predicted for the momentum distribution of the D^+ events as shown in the lower right graph of Fig. 3. The striking difference between the two model predictions at large x_f underscores the crucial role played by the χ distribution in determining the production asymmetry in the context of string fragmentation. When most of the target nucleon energy is partitioned to the diquark, as is the case for Model 1, the x_f spectrum for D^- is significantly hardened compared to that for D^+. The D^+ tends to be fragmented closer in rapidity to its string partner–the diquark–which in this case tends to be at a more negative center of mass rapidity than the bachelor quark. On the other hand, when the energy is divided more evenly, which is characteristic of Model 2, the resulting D^- and D^+ x_f distributions are more similar. In fact, when the χ distribution is fixed to a value of 0.5 the asymmetry nearly vanishes in each of the kinematic variables plotted in Fig. 3. Similar findings result for the other D meson decay modes although our data sample lacks sufficient statistics to meaningfully subdivide the D_s^+ and Λ_c^+ samples.

To further test the two models considered here, we repeated our measurements for charm candidates produced in association with a partially reconstructed D^{*-}. We used the same semi-inclusive technique described in our earlier article which studied correlations between $D\overline{D}$ pairs [12]. Briefly, a fully reconstructed charm meson (which we call the recoil charm

D_r) is produced against a kinematically tagged soft pion of the correct charge (which we label as $\tilde{\pi}$) from the decay $D^{*-} \to \tilde{\pi}^- \overline{D^0}$ where the daughter $\overline{D^0}$ need not be reconstructed. Because of the low Q value for this decay, the soft pion will have a lab momentum close to that of the parent D^{*-} when scaled up by the inverse of its energy fraction (approximately 13.8). Since fully reconstructed $D\overline{D}$ pairs balance p_t^2 within 4 (GeV/c)^2 at these photon beam energies (as shown in Fig.2a of Ref [12]), the scaled soft pions from the D^{*-} decay should roughly balance the recoil charm transverse momentum, $\vec{p_t}^{\,r}$. Therefore, one expects an excess in signal $\tilde{\pi}$'s over background pions below $\tilde{\Delta}_t^2 = 4$ (GeV/c)^2 where

$$\tilde{\Delta}_t^2 \;\; = \;\; (13.8 p_x^{\pi} + p_x^r)^2 + (13.8 p_y^{\pi} + p_y^r)^2. \qquad (4)$$

Using our sample of D_r mesons (which include D^+, D^{*+} and D^0) $\tilde{\Delta}_t^2$ is computed for each track emanating from the primary vertex. Fig. 4(a) shows $\tilde{\Delta}_t^2$ for candidates having the correct charge correlation and the wrong charge correlation for the D_r sample** where we additionally have performed a subtraction for background events beneath the D_r mass peaks. In the present work we have expanded our analysis to search for D_s^+ and Λ_c^+ candidates produced opposite a D^{*-}. Applying the same technique as for the D_r events, the analogous $\tilde{\Delta}_t^2$ distributions for these candidates are shown in Figs. 4(b,c). The accumulated excesses in these distributions below $\tilde{\Delta}_t^2 = 4$ (GeV/c)^2 correspond to reconstructed samples of approximately 4500 events due to $\tilde{D}^{*-} D$ production, 75$\pm$27 events due to $\tilde{D}^{*-} D_s^+$ production and 120$\pm$45 events due to $\tilde{D}^{*-} \Lambda_c^+$ production (charge conjugates included) where the symbol $\tilde{D}^{*-}$ denotes the partially reconstructed D^{*-} using the soft pion $\tilde{\pi}$ tag.

The measured photoproduction asymmetries for the charm species produced in association with a $\tilde{D}^{*-}$ are listed in Table III and are compared to the predictions from the two Monte Carlo models. To compute the asymmetry we have separately accumulated the excess

---

**We remove pions consistent with the decay $D^{*+} \to \pi D_r^0$ by eliminating those wrong-charge candidates lying within 3 MeV of the nominal $D^{*+} - D_r^0$ mass difference.

below $\tilde{\Delta}_t^2 = 4$ $(\mathrm{GeV/c})^2$ for the two charge states. Explicitly, our definition[††] for this type of asymmetry is

$$\alpha = \frac{N(\tilde{D}^{*-}\ c) - N(\tilde{D}^{*+}\ \overline{c})}{N(\tilde{D}^{*-}\ c) + N(\tilde{D}^{*+}\ \overline{c})}. \tag{5}$$

As before, the Monte Carlo events were subjected to the same apparatus conditions, event selection criteria, analysis cuts (as well as counting techniques) as were the data and therefore correspond to the same region of kinematic variables. Observation of a non-zero asymmetry in $\tilde{D}^{*-}D$ events, which therefore exclude contributions from charm baryon production, would provide direct evidence for a kinematic asymmetry. However, the weighted average of the five $\tilde{D}^{*-}D$ asymmetries of Table III is only 2.7σ different from zero. For almost all of the event types our measurements are not of sufficient statistical strength to discriminate between the two models. For two of the modes we have illustrated χ^2 contours corresponding to $1-3\sigma$ deviations from our reported values in terms of the measured total event yield and asymmetry (Fig. 5). For the highest statistics mode $\tilde{D}^{*-}D^+$, our measurement is in good agreement with the prediction from Model 2 while it is consistent with Model 1 at the 3σ level; this result is in parallel to the results for inclusively produced D^+ events. It is interesting that for the $\tilde{D}^{*-}\Lambda_c^+$ events (the only type containing a charm baryon) our data is in better agreement with the prediction from Model 1 while the Model 2 prediction is lower than our observation by 2.86σ.

In summary, we observe statistically significant enhancements of $\overline{D}$ over D production in the kinematic region characterized by $E_\gamma \simeq 200$ GeV which cannot be attributed to an apparatus asymmetry. As a measure of the statistical significance of these results, our measurement for the inclusive production asymmetry combining the D meson modes within our acceptance is $\alpha = -3.7 \pm 0.6\%$ corresponding to more than 6 standard deviations from zero. The kinematic dependence exhibited by our inclusive asymmetry measurements

---

[††]A negative value of α for the $\tilde{D}^{*-}D^+$ entry of Table III, for example, means $\tilde{D}^{*+}D^-$ events predominate over $\tilde{D}^{*-}D^+$ events.

is well reproduced by the Lund fragmentation model when the assumed distribution for the momentum fraction χ carried by the bachelor quark is hard ("Model 2"). While our inclusive asymmetry measurements agree in sign with both models, the values are smaller in magnitude and exhibit less kinematic dependence than those in the model where the χ distribution is sharply peaked near zero ("Model 1"). At our energies we observe no significant excess of D_s^+ over D_s^- or Λ_c^+ over Λ_c^-. The situation for our semi-inclusive measurements for charm states produced against a $D^{*\pm}$ meson is less clear. Our highest statistics sample $D^{*-}D^+$ favors the hard χ distribution while the much smaller $D^{*-}\Lambda_c^+$ sample is inconsistent with this model at the 2.86σ level.

We thank T. Sjöstrand for helpful discussions. We wish to acknowledge the assistance of the staffs of the Fermi National Accelerator Laboratory, the INFN of Italy, and the physics departments of the collaborating institutions. This research was supported in part by the National Science Foundation, the U.S. Department of Energy, the Italian Istituto Nazionale di Fisica Nucleare and Ministero dell'Università e della Ricerca Scientifica e Tecnologica, and the Korean Science and Engineering Foundation.

REFERENCES

[a] Present address: Fermilab, Batavia, IL 60510, USA.

[b] Present address: University of Maryland, College Park, MD 20742, USA.

[c] Present address: University of South Carolina, Columbia, SC 29208, USA.

[d] Present address: Vanderbilt University, Nashville, TN 37235, USA.

[e] Present address: Enrico Fermi Institute, University of Chicago, Chicago, IL 60637, USA.

[f] Present address: Syracuse University, Syracuse, NY 13244-1130 , USA.

[g] Present address: University of Colorado, Boulder, CO 80309, USA.

[h] Present address: State University of New York at Stony Brook, Stony Brook, NY 11794-3800, USA.

[i] Present address: AT&T Bell Labs, West Long Branch, NJ 07764, USA.

[j] Present address: Pohang Accelerator Laboratory, Pohang, Korea.

[k] Present address: Lawrence Berkeley Laboratory, University of California, Berkeley, CA 94720, USA.

[l] Present address: Science Applications International Corporation, McLean, VA 22102, USA.

[m] Present address: Gamma Products Inc., Palos Hills, IL 60465, USA.

[1] L.M. Jones and H.W. Wyld, Phys. Rev. D 17 (1978) 759.

[2] R.K. Ellis and P. Nason, Nucl. Phys. B 312 (1989) 551.

[3] J. Smith and W.L. van Neerven, Nucl. Phys. B 374 (1992) 36.

[4] S. Frixione, M. Mangano, P. Nason, G. Ridolfi, Nucl. Phys. B 412 (1994) 225.

[5] T.Sjöstrand, Computer Phys. Comm. 39 (1986) 347;

T.Sjöstrand, M.Bengtsson, Computer Phys. Comm. 43 (1987) 367;

H.-U.Bengtsson, T.Sjöstrand, Computer Phys. Comm. 46 (1987) 43.

[6] T. Sjöstrand, PYTHIA 5.6 and JETSET 7.3: Physics and Manual, CERN-TH.6488/92 (1992).

[7] SLAC Hybrid Facility Photon Collab., K. Abe *et al.*, Phys. Rev. D 33 (1986) 1.

[8] C. Peterson, D. Schlatter, I. Schmitt and P. Zerwas, Phys. Rev. D27 (1983) 105.

[9] E687 Collab., P.L. Frabetti *et al.*, Nucl. Instrum. Methods. A 320 (1992) 519;
E687 Collab., P.L. Frabetti *et al.*, Nucl. Instrum. Methods. A 329 (1993) 62.

[10] Particle Data Group, L. Montanet *et al.*, Phys. Rev. D 50 (1994).

[11] The Monte Carlo program consisted of simulation algorithms for the E687 apparatus (Ref. [9]) combined with the Lund model packages JETSET 7.3 and PYTHIA 5.6 (Ref. [6]).

[12] E687 Collab., P.L. Frabetti *et al.*, Phys. Lett. B 308 (1993) 193.

[13] E691 Collab., J.C. Anjos *et al.*, Phys. Rev. Lett. 62 (1989) 513.

[14] NA14/2 Collab., M.P. Alvarez *et al.*, Z. Phys. C 60 (1993) 53.

FIGURES

FIG. 1. A schematic representation of the color poles and strings for the case of fixed-target photoproduced charm quarks in the context of the Lund string fragmentation model (top), and an example of hadron formation as a result of string breaking (bottom). Q labels the "diquark" from the target nucleon and q labels the "bachelor quark".

FIG. 2. Invariant mass distributions and approximate event yields ("Y") for the D meson, the D_s^+ meson, and the Λ_c^+ baryon candidates used in this analysis (particles and antiparticles have been combined). For the D meson states we combine all decay modes and plot the normalized mass variable $\Delta M/\sigma$, where ΔM is the difference between the reconstructed mass (with error σ) and the Particle Data Group value for the candidate. For the combined D meson sample we also indicate the relative efficiency as a function of x_f of all apparatus acceptance and analysis cuts (very little variation is exhibited in p_t^2).

FIG. 3. Kinematic variations of the production asymmetry α as a function of p_t^2, E_γ and x_f for the decay mode $D^+ \to K^-\pi^+\pi^+$ from this experiment (data with error bars) and the two Monte Carlo predictions discussed in the text (solid lines from Model 1, dashed from Model 2). The lower right figure compares the two model predictions for the D^+ momentum (P) to the data.

FIG. 4. Distribution of the p_t balance variable $\tilde{\Delta}_t^2$ for soft $\tilde{\pi}$-tagged charm mesons and baryons. The crossed points are for events in which the $\tilde{\pi}$ has the right sign charge correlation and the diamond points are for the wrong sign charge correlation. For the high statistics sample of $\tilde{\pi}$-tagged D mesons shown in graph a), the solid curve overlaying the right sign excess, which is attributed to $D^{*-}D$ production, is from Ref. 12 and represents a comparison to expectations (accounting for resolution effects) for a fully reconstructed $D\overline{D}$ sample, while the dashed curve is a fit to the wrong sign distribution. In the (statistically weaker) $\tilde{\pi}$-tagged D_s^+ and Λ_c^+ samples shown in graphs b) and c), the solid and dashed curves are predictions (area normalized) for the right and wrong sign charge correlations respectively from the Lund Monte Carlo (Model 1); the right sign excess observed in data is attributed to $D^{*-}D_s^+$ and $D^{*-}\Lambda_c^+$ production (charge conjugates have been combined in all of these figures).

FIG. 5. Contours for χ^2 deviations of $1-3\sigma$ from the reported measurements (black dots) as a function of the total yield of charm candidates produced in association with a D^{*-} and the measured asymmetry for a) $\tilde{D}^{*-}D^+$ and b) $\tilde{D}^{*-}\Lambda_c^+$ event types. The distortion of the contour due to low $\tilde{D}^{*-}\Lambda_c^+$ event statistics is evident.

TABLES

TABLE I. Production asymmetry α (%) from this experiment compared to two Monte Carlo predictions based on the Lund model [11].

Decay mode	E687 (This exp.)	Model 1	Model 2
$D^+ \to K^-\pi^+\pi^+$	-3.8 ± 0.9	-10.4 ± 0.4	-2.9 ± 0.3
$D^{*+} \to D^0\pi^+ \to (K^-\pi^+)\pi^+$	-6.4 ± 1.5	-9.2 ± 0.7	-2.4 ± 0.5
$D^{*+} \to D^0\pi^+ \to (K^-\pi^+\pi^+\pi^-)\pi^+$	-4.0 ± 1.7	-9.2 ± 0.8	-3.0 ± 0.5
$D^0 \to K^-\pi^+$ (no D^*-tag)	-2.0 ± 1.5	-5.1 ± 0.6	-1.6 ± 0.4
$D^0 \to K^-\pi^+\pi^+\pi^-$ (no D^*-tag)	-1.9 ± 1.5	-9.9 ± 0.5	-2.9 ± 0.4
$D_s^+ \to K^-K^+\pi^+$	2.5 ± 5.2	9.7 ± 1.7	2.5 ± 0.7
$\Lambda_c^+ \to pK^-\pi^+$	3.5 ± 7.6	21.5 ± 0.7	-7.7 ± 0.6

TABLE II. Antiparticle/particle production ratios $R = N_{\bar{c}}/N_c$ from this experiment and from the Tagged Photon Collaboration (E691).

Decay mode	E687 (This exp.) $< E_\gamma > \simeq$ 200 GeV	E691 [13] $< E_\gamma > \simeq$ 120 GeV
$D^+ \to K^-\pi^+\pi^+$	1.08 ± 0.02	1.04 ± 0.03
$D^{*+} \to D^0\pi^+ \to (K^-\pi^+)\pi^+$	1.13 ± 0.03	1.15 ± 0.07
$D^{*+} \to D^0\pi^+ \to (K^-\pi^+\pi^+\pi^-)\pi^+$	1.08 ± 0.04	1.23 ± 0.07
$D^0 \to K^-\pi^+$ (no D^*-tag)	1.04 ± 0.03	1.08 ± 0.03
$D^0 \to K^-\pi^+\pi^+\pi^-$ (no D^*-tag)	1.03 ± 0.03	
$D_s^+ \to K^-K^+\pi^+$	0.95 ± 0.10	0.92 ± 0.14
$\Lambda_c^+ \to pK^-\pi^+$	0.93 ± 0.14	0.79 ± 0.17

TABLE III. Production asymmetry α (%) for candidates produced in association with a $D^{*\pm}$ (see text for explicit definition).

$\gamma N \to$ (Decay mode) D^{*-}	E687 (This exp.)	Model 1	Model 2
$D^+ \to K^-\pi^+\pi^+$	-12 ± 5.1	-28 ± 4	-7.2 ± 1.6
$D^{*+} \to D^0\pi^+ \to (K^-\pi^+)\pi^+$	-9.6 ± 8.9	-25 ± 5	-3.4 ± 2.4
$D^{*+} \to D^0\pi^+ \to (K^-\pi^+\pi^+\pi^-)\pi^+$	8.6 ± 14	12 ± 3.9	-10 ± 2.9
$D^0 \to K^-\pi^+$ (no D^*-tag)	5 ± 21	-30 ± 8.8	-6.5 ± 3.8
$D^0 \to K^-\pi^+\pi^+\pi^-$ (no D^*-tag)	-38 ± 16	-39 ± 7.2	-13 ± 3.2
$D_s^+ \to K^-K^+\pi^+$	51 ± 42	45 ± 6.9	5.5 ± 3.1
$\Lambda_c^+ \to pK^-\pi^+$	83 ± 49	73 ± 3.1	-33 ± 2.8

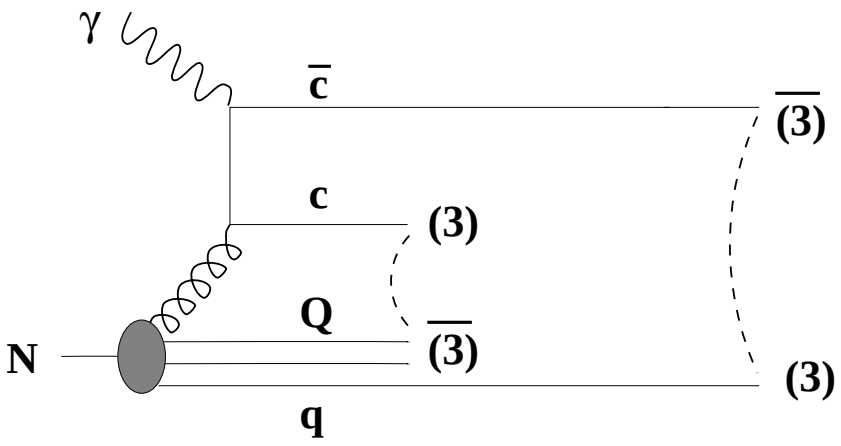
γ
c̄
(3)̄
c
(3)
Q
(3)̄
N
(3)
q

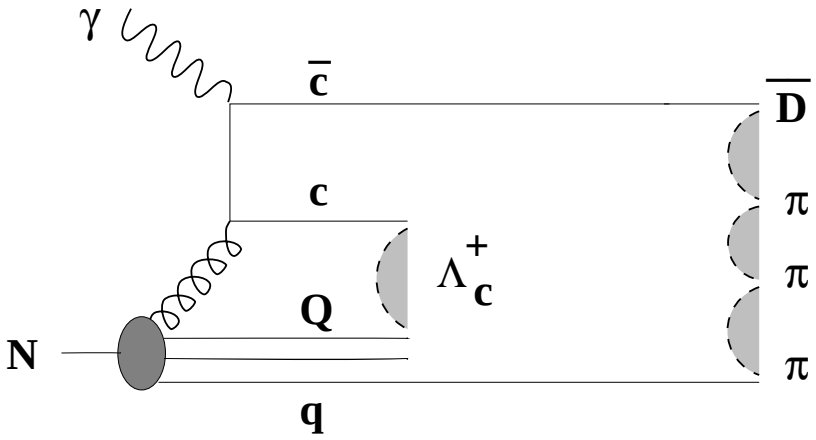
γ
c̄
D̄
c
π
Λ+c
π
Q
N
π
q

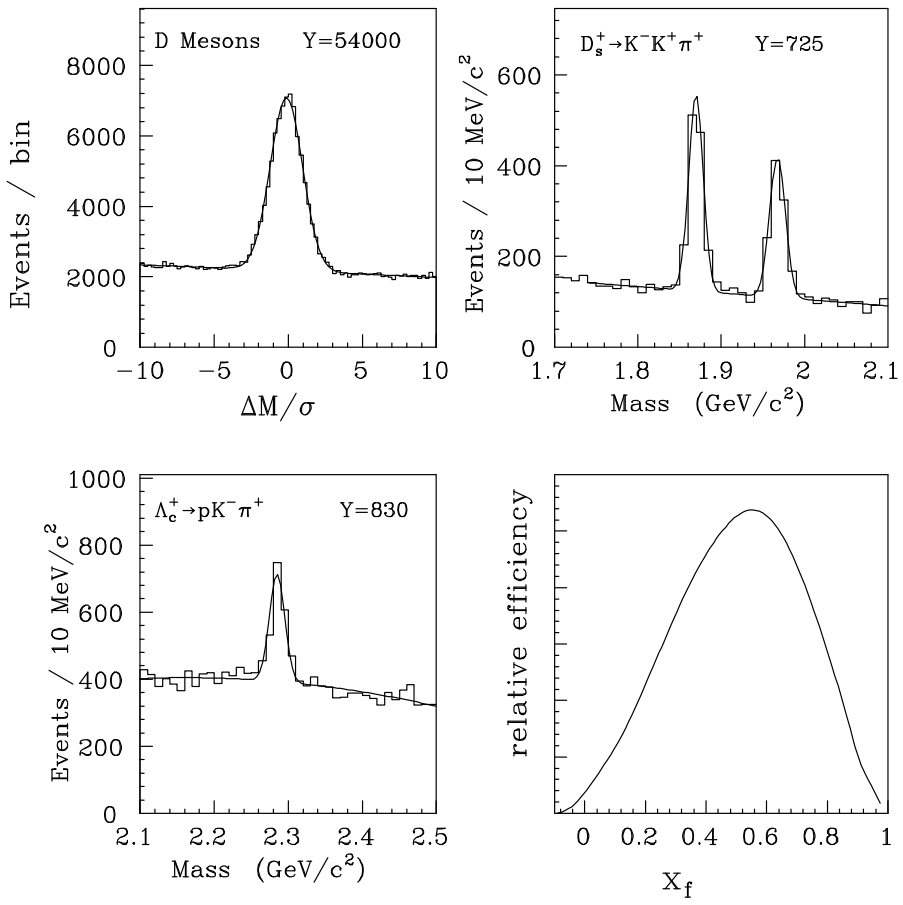
D Mesons Y=54000
Events / bin
ΔM/σ
$D_s^+ \to K^- K^+ \pi^+$ Y=725
Events / 10 MeV/c^2
Mass (GeV/c^2)
$\Lambda_c^+ \to pK^- \pi^+$ Y=830
Events / 10 MeV/c^2
Mass (GeV/c^2)
relative efficiency
X_f

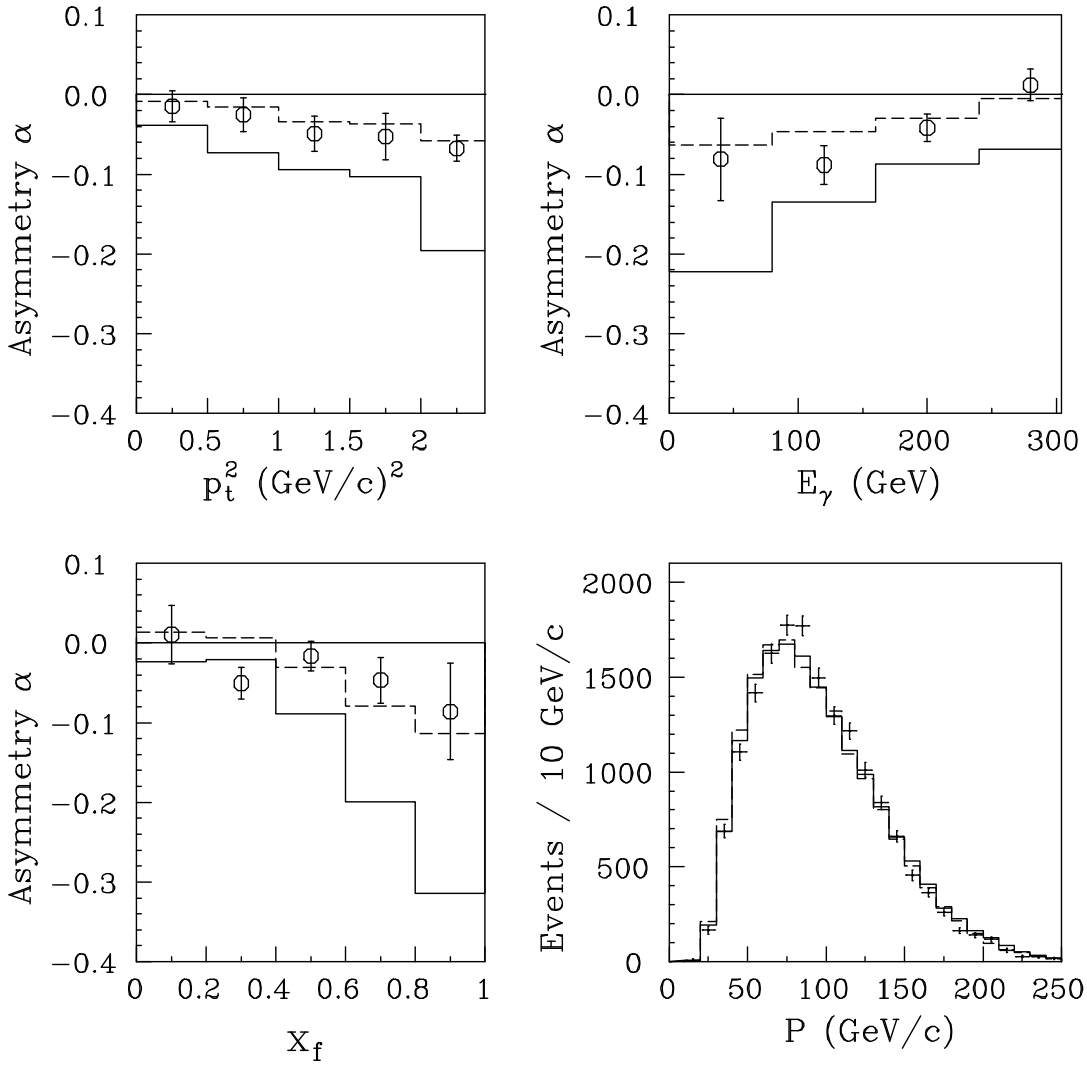
Asymmetry α
0.1
0.0
−0.1
−0.2
−0.3
−0.4
0
0.5
1
1.5
2
p_t^2 (GeV/c)^2
Asymmetry α
0.1
0.0
−0.1
−0.2
−0.3
−0.4
0
100
200
300
E_γ (GeV)
Asymmetry α
0.1
0.0
−0.1
−0.2
−0.3
−0.4
0
0.2
0.4
0.6
0.8
1
x_f
Events / 10 GeV/c
2000
1500
1000
500
0
0
50
100
150
200
250
P (GeV/c)

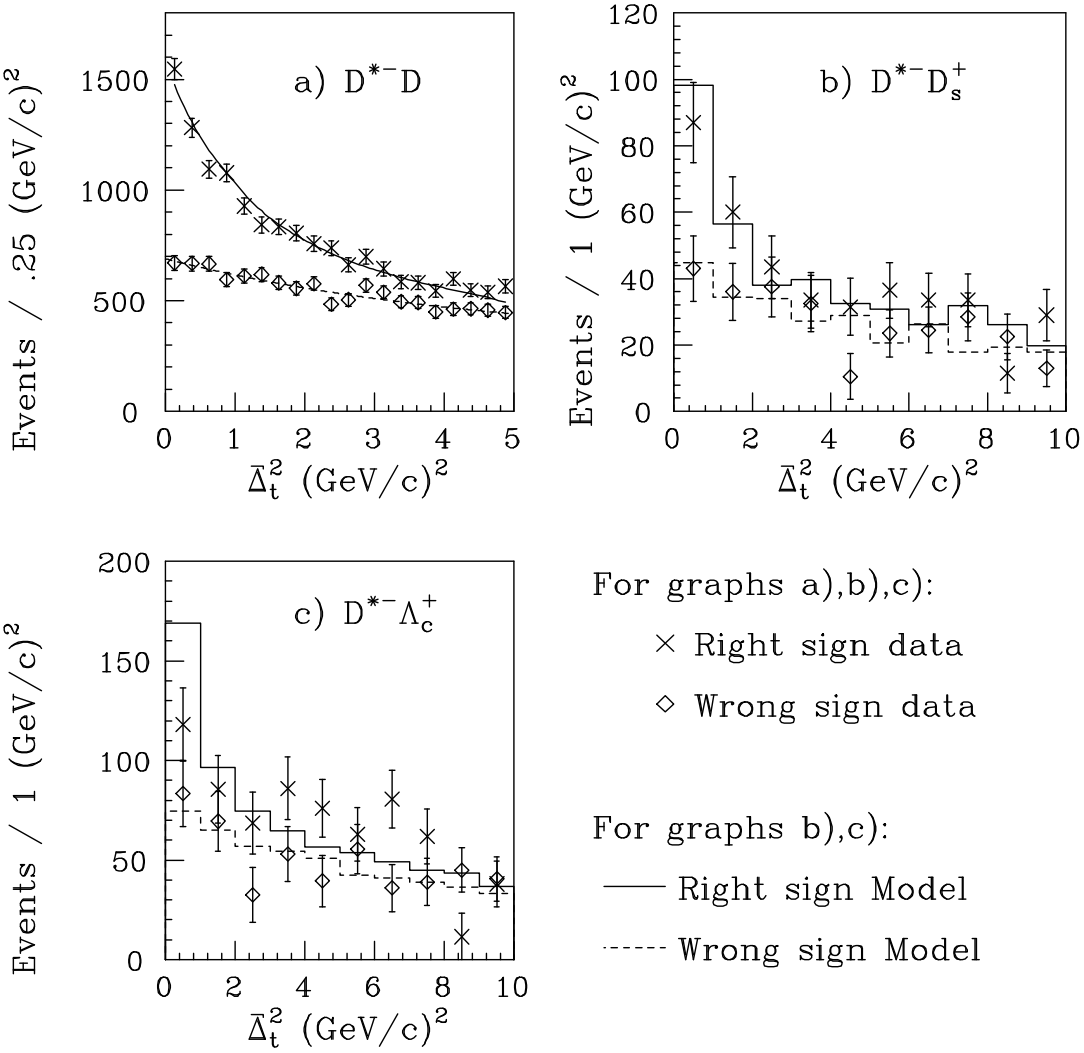
a) $D^{*-}D$
b) $D^{*-}D_s^+$
c) $D^{*-}\Lambda_c^+$
Events / .25 (GeV/c)^2
Events / 1 (GeV/c)^2
$\bar{\Delta}_t^2$ (GeV/c)^2
For graphs a),b),c):
× Right sign data
◇ Wrong sign data
For graphs b),c):
Right sign Model
Wrong sign Model

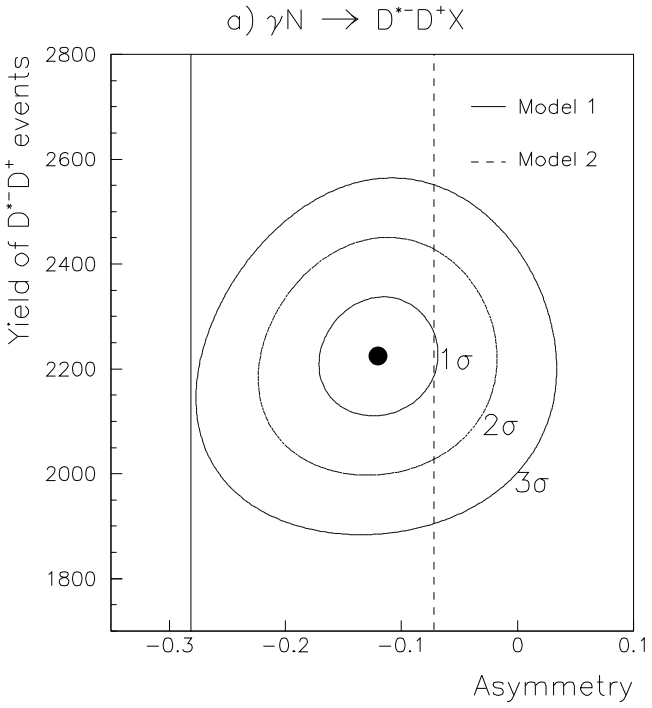
a) γN → D*⁻D⁺X
Yield of D*⁻D⁺ events
Asymmetry
Model 1
Model 2
1σ
2σ
3σ
2800
2600
2400
2200
2000
1800
−0.3
−0.2
−0.1
0
0.1

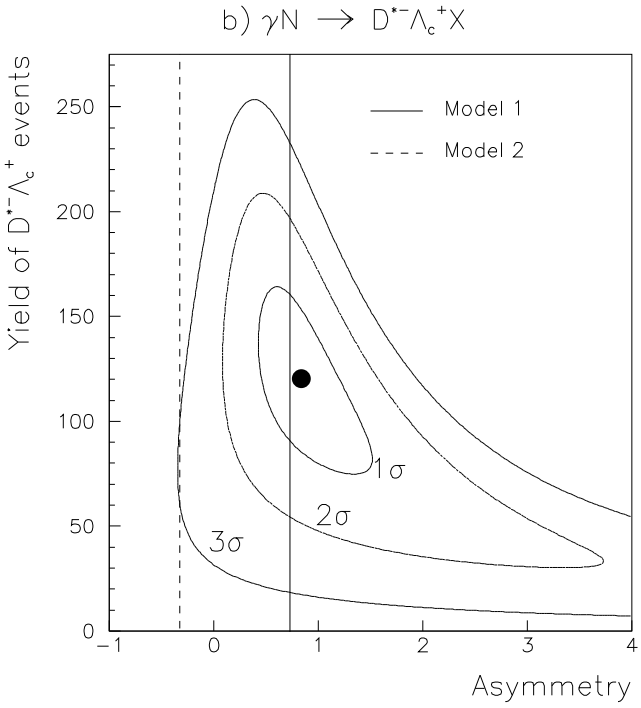
b) γN → D*⁻Λc⁺X
Yield of D*⁻Λc⁺ events
Asymmetry
Model 1
Model 2
1σ
2σ
3σ
250
200
150
100
50
0
−1
0
1
2
3
4